論 文

Effects of Control Factors on the Morphology of Compacted/Vermicular Graphite.(I)

Byung-Joon Ye

C/V 흑연의 형상에 미치는 공정요소의 영향(I)

예 병 준

개 요

C/V 흑연 주철의 흑연형상에 미치는 응고인자(control factor)들의 영향을 조사하기 위해 첨가제, holding time과 열처리의 유무등을 변화시켜 보았다. 이때 흑연형상의 척도로서 길이/폭의 비를 사용하였으며, 단면적의 감소는 구상흑연의 증가와 더불어 이 비율의 증가가 확인되었으나 현격한 변화라고 단정 지을 수는 없었다. Mg-Ti합금과 Rare earth silicides의 첨가에 따라 다른 미세조직이 관찰되었으나 이 또한 기지조직의 차이에 의한 것이었고 실제 흑연의 형상에는 영향이 없었다. 4, 5분의 유지 시간으로는 흑연형상의 변화를 감지할 수 없었으며, 탄소/실리콘의 변화도 기지조직 이외에는 변화를 일으키지 않았다. 소둔 열처리의 경우 Rare earth를 첨가한 13mm 직경의 경우만 C/V 흑연이 약간 두꺼워졌을 뿐 대체로 괄목할 만한 차이가 확인되지 못했다.

To see the change in the morphology of compacted graphite, a solidification factor-treatment for C/V graphitization and holding time for fading effect-and heat treatment were studied in this research.

1. Introduction

Compacted/vermicular graphite was introduced due to the properties of compacted graphite cast iron such as high tensile strength with high thermal conductivity and good machinability.[1,2)]

It is well known that the major properties of cast iron depend upon the shape of graphite. The high tensile strength and ductility of ductile iron come from the spheroidal morphology of the graphite. The good thermal conductivity and good machinability of gray cast iron come from flake shaped graphite.

Different treatment for compacted/vermicular graphitization may result the morpholgy in another trend mainly because of their different fading characteristic.[3,4,5)] The diffusivity and the tendency of the matrix change could be checked when the specimen is heated to the austenitic region.

2. Experimental Procedures

2.1 Objectives

The objective of this study was to determine the effects of several variables which may affect the morphology of compacted graphite. Thcse variables are as follows :

1. Different treatment for compacted/vermicular graphitization.
2. Holding time after inoculation and post inoculation.
3. Effect of heat treatment.

2.2 Molding and Heat Procedure

All of the molds for this study were air set molds. Three different section size(13mm, 25mm,

경북대학교 금속공학과(Department of Metallurgical Engineering, Kyungpook National University)

38mm) round bars were poured simultaneously. The length of the bars was 150mm.

Mg-treatment or rare earth silicide treatment was done between 1,454C and 1,538C during the process of pouring melts to the ladle to take advantage of quick mixing.

Post inoculation followed the treatment in a few seconds. Each time, after the treatment and after post inoculation, the melt was stirred with a steel rod. Then a eutectometer cup and a chemical analysis sample were poured.

About 30 seconds later, after post inoculation, the first series of three different section sizes was poured. After waiting 2 minutes holding the melt in the ladle, another set of samples was poured.

2.3 Charge Calculation

The charge for the 45.3kg induction furnace heats was composed of ductile iron sprue and steel scrap in the proper proportions to bring about the desired silicon content of the heats. Taking into account carbon losses during melting, carbon raiser was added to the melt for the proper carbon content.

The Chemical analyses of ductile iron sprue, steel scrap and carbon raiser are listed in Table 1. Also, nominal chemical analyses of rare earth silicide and ferrosilicon for post inoculation are listed in Table 1.

Typical charge calculations would be as follows :

a. Rare Earth Treated

1. Desired carbon equivalent : 4.40%
2. Total silicon : 1.80%
3. Total carbon : 4.40−1.80/3=3.80%
4. Silicon gain from 0.25% rare earth silicide : 0.4% × 30% =0.12%
5. Silicon gain from post inoculation : 0.5% × 75% =0.38%
6. Silicon supply from ductile iron sprue : 1.80−(0.12+0.38)=1.30%
7. Ductile iron sprue needed : (1.30/2.5)×45.3kg=23.6kg
8. Steel scrap needed : 21.7kg
9. Expected carbon loss during melting : 0.3%
10. Total carbon necessary : 3.8+0.3=4.1%
11. Carbon raiser necessary : 4.1−(23.6/45.3×0.035+21.7/45.3×0.002)×100=2.18%

This example charge calculation is shown in Table 2. In the case of the C 3.4%/Si 3.0% heats, the calculations which are different from the calculations above would be as follows :

2. Total silicon : 3.0%
3. Total carbon : 4.40−3.0/3=3.40%
6. Silicon supply from ductile iron sprue : 3.0−(0.12+0.38)=2.50%
7. Ductile iron sprue needed : (2.50/2.50)×45.3*kg*

Table 1. Nominal analysis of charge materials and additions

Material	Composition						
Ductile Iron Sprue	C 3.5−3.7	Si 2.2−2.6	Mn 0.3−0.35	S 0.01	P 0.02	Mg 0.05	Fe Bal.
Steel Scrap	0.2	0.1	0.4	—	—	—	Bal.
Carbon Raiser	C 98.5	Si 0.27	SiO_2 0.03	Fe 0.0045	H_2O 0.02	Ash 0.5	Others V 0.005 Ni 0.0002
Rare Earth Silicide	Ce 16.46	La 9.88	Other RE 6.58	Ca 0.41	Al 0.25	Si 33.2	Fe 32.2
Ferrosilicon	—	—	—	0.8	1.0	75.0	23.2

Table 2. Example charge calculation of 45.3kg melt

Materials	Amount(kg)	Carbon(%)	Silicon(%)
D. I. Sprue	34.4	2.66	1.30
Steel Scrap	10.9	0.05	—
RE Silicide	0.18	—	0.12
Post Inoculation	0.23	—	0.38
Carbon Loss	—	−0.30	—
Carbon Raiser	—	1.39	—
Total	45.7	3.80	1.80

Table 3. Targets of heats poured with different treatment and different carbon-silicon ratio

A. Mg-Ti Alloy Treated						
Heat No.	C*	Si*	Mg	S	P	C.E. Aimed
1	3.8	1.8	0.01−0.02	0.05	0.05	4.4
2	3.7	2.1	0.01−0.02	0.05	0.05	4.4
3	3.6	2.4	0.01−0.02	0.05	0.05	4.4
4	3.5	2.7	0.01−0.02	0.05	0.05	4.4
5	3.4	3.0	0.01−0.02	0.05	0.05	4.4
B. Rare Earth Silicide Treated						
Heat No.	C*	Si*	Ce	S	P	C.E. Aimed
6	3.8	1.8	0.02	0.05	0.05	4.4
7	3.7	2.1	0.02	0.05	0.05	4.4
8	3.6	2.4	0.02	0.05	0.05	4.4
9	3.5	2.7	0.02	0.05	0.05	4.4
10	3.4	3.0	0.02	0.05	0.05	4.4

* Checked with the eutectic arrest temperatures representing C.E.

8. Steel scrap needed : none

10. Total carbon necessary : 3.4+0.3=3.7%

11. Carbon raiser necessary : 3.7−(0.035×100lb)= 0.2%

b. Mg-Ti alloy treated

The same process was used except the silicon gain from Mg-Ti alloy was considered instead of the rare earth silicide.

In this case, the calculation could be as follows : 1.2% of Mg-Ti alloy × 50% of silicon in the alloy = 0.6% silicon added by Mg-Ti alloy treatment.

The target chemical compositions of each heat based on the above charge calculation are shown in Table 3.

2.4 Experimental Design

Five major factors as shown below were considered in the design of this experiment.

1. Two different kinds of treatment.
2. Three different holding time in the pouring.
3. Heat treatment.

2.5 Sample Preparation and Examination

To avoid the end chill effect, the section to be polished was chosen at the place shown in Fig. 1. The bar shaped samples as cast and after annealing were cut by a metallographic cut off machine.

Specimens for optical microscopy were obta-

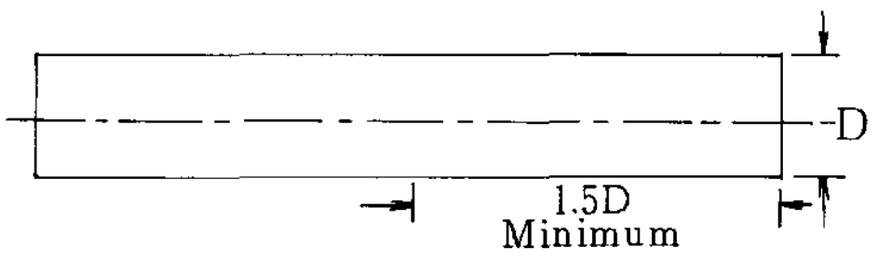

Fig. 1 Section selection, 1.5 X diameter far from one side of a bar

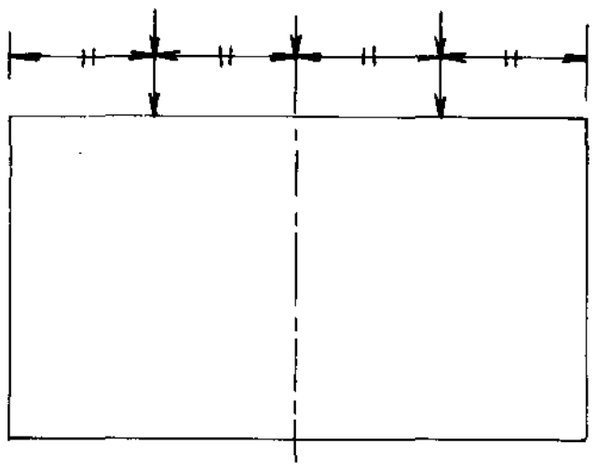

Fig. 2 Places for optical microscope between edge and center of a bar

ined from the approximate mid-section between the center of the bar and the edge of the bar as shown in Fig. 2.

The samples of 13mm and 38mm section sizes were left unmounted to check the difference between inner and outer microscopy of a section.

Those samples were polished using standard metallographic techniques.

2.6 Percent Spheroidal Graphite Measurement

To measure percent spheroidal graphite, a metallographic microscope was used. Projecting the image of the polished specimen onto a ground glass plate at 200X, the number of spheroidal graphite of type I and type II in the image area of 10cm×10cm which corresponds to a 0.25 sq.mm. sample area(0.5mm×0.5mm) was counted as one group and the total number of graphite particles in the same area was counted as the other group. Four counts were taken and averaged.

Percent spheroidal graphite was then measured as follows :

$$\text{Percent Spheroidal Graphite} = \frac{\text{No. of type I, II nodules}}{\text{Total number of graphites}}$$

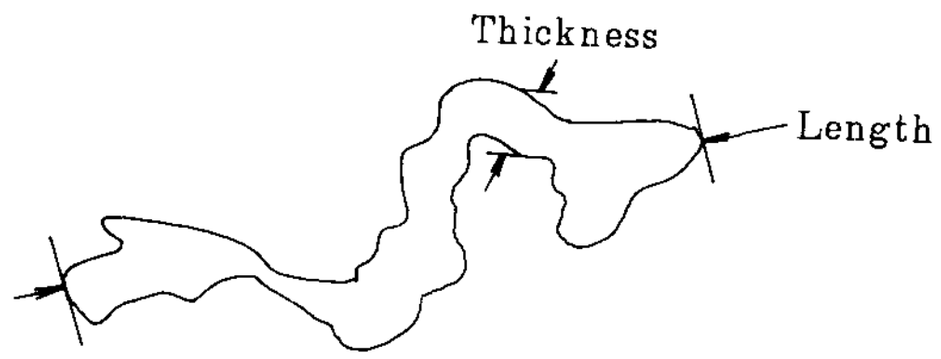

Fig. 3 Typical method of thickness-length ratio measurement

2.7 Thickness-Length Ratio Measurement

The thickness-length ratio of compacted graphite measurement was made at the same time as the percent spheroidal graphite measurement.

A typical method of measuring the thickness -length ratio of compacted graphite is shown in Fig. 3.

Four counts were taken. One was chosen among typical short and thick compacted graphite. Another was chosen among typical thin and long compacted graphite. The other two were chosen among moderate compacted graphite. Then all four were averaged.

3. Experimental Results

Fig. 4 shows the relationship of holding time and percent spheroidal graphite with different treatment and different section sizes. Another result which shows the effect of holding time on the thickness-length ratio of compacted graphite is shown in Fig. 5. The effect of holding time up to 4.5 minutes is not significant as shown in Fig. 4 and 5.

Fig. 6, 7 and 8 show the microstructures of compacted graphite cast irons as cast and annealed. The microstructures at the top of each figure are as cast and those at the bottom are after annealing. All photographs of 13mm and 25mm section size were taken at the magnification of 150, but those of 38mm were taken at the magnification of 75 because of too large graphite and matrix under investigation for the

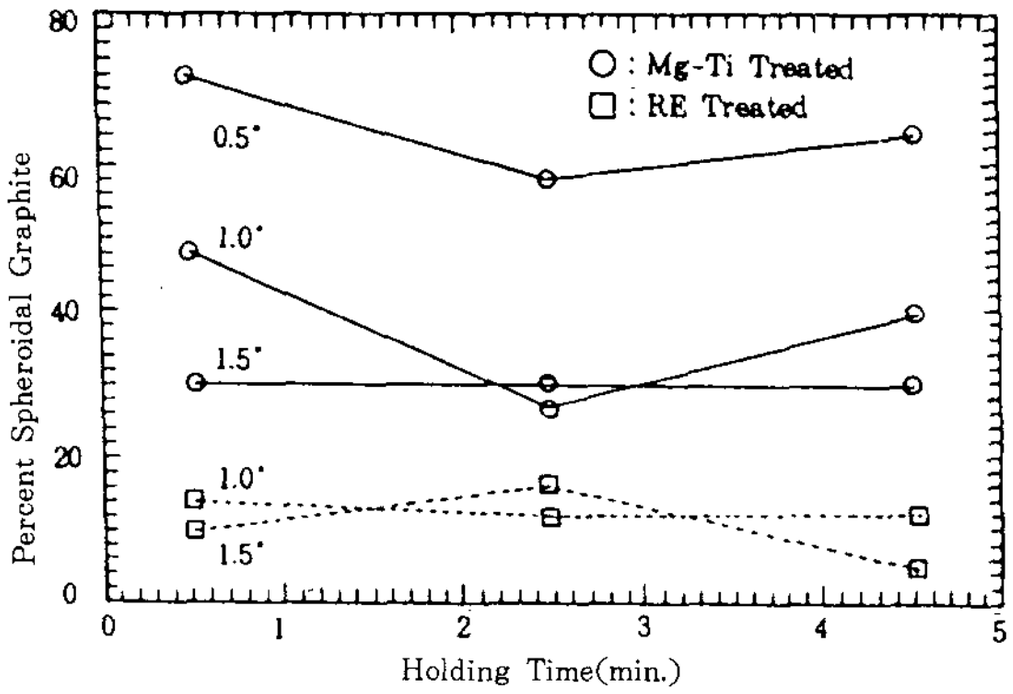

Fig. 4 Holding time and percent spheroidal graphite

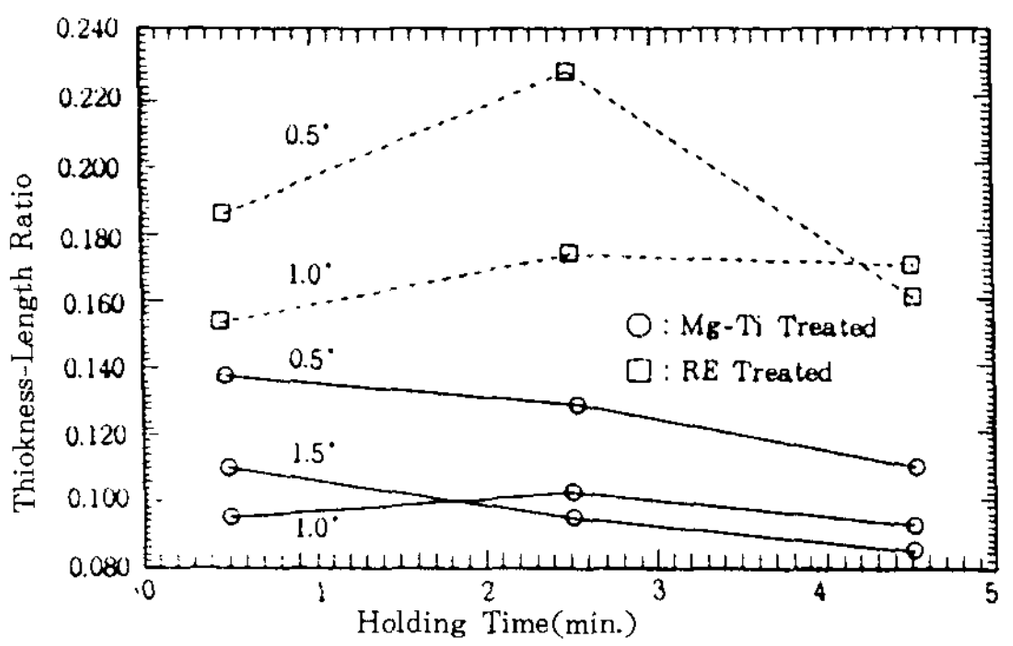

Fig. 5 Effect of holding time on the thickness-length ratio with different section size and treatment

frame of the photographs. This effect of heat treatment of 13mm section size is more significant than that of 25mm and 35mm section size.

4. Discussion

As written in the experimental procedure the samples were poured at 0.5 minutes, 2.5 minutes and 4.5 minutes after post inoculation. This was not a long enough time to observe significant differences occuring in the morphology of compacted graphite. Therefore Fig. 4 shows that no significant difference occurs in the percent spheroidal graphite at 4.5 minutes of holding time. Fig. 5 also shows that there is no significant difference in the thickness-length ratio of compacted graphite.

Fig. 6, 7 and 8 show evidences of this phenomenon. No significant difference in the morphology of compacted graphite could be found by comparing figures above which have the same conditions-treatment, carbon/silicon ratio and section size.

The typical matrix in a medium section size which contains compacted graphite is pearlite and ferrite. But carbide can dominate pearlite and ferrite by rapid cooling in a thinner section as shown in Fig. 6 and 8. In a thicker section, 38mm or more, ferrite is the major matrix constituent in the microstructures as shown in Fig. 7 and 8.

Heating the samples up to 871 C, the matrix of those samples consists more of austenite and carbide. By slow cooling in the furnace, the matrix easily forms ferrite and carbide. In thin sections as shown in Fig. 6, 7 and 8, all of the pearlite in the matrix was changed to ferrite.

The carbon in pearlite could be diffused in austenite when the temperature is above the A_1 line in the Fe-C phase diagram. With slow cooling in the furnace carbon component segregates in the form of graphite. But no noticeable difference could be detected in the shape, the scale and the amount of graphite with two exceptions. These two cases are shown in Fig. 6(C 3.4/Si 3.0, 13mm section size, 0.5 min. holding time) and Fig. 14(C 3.4/Si 3.0, 13mm, 4.5 min.). In these two cases, the excessive carbide transforms to austenite during the heating procedure. Then carbon composition in austenite becomes graphite by the formation of ferrite in the matrix and it segregates independently or is added to the already existed graphite. Graphite addition occurred along the grain boundary as shown in Fig. 6.

In thicker sections as shown in Fig. 7 and 8, the microstructures of the Mg-Ti alloy treated cast iron as shown in Fig. 7 show no major difference in matrix and graphite morphology before and after annealing.

		Mg-Ti Alloy Treated	Rare Earth Silicide Treated
C/Si Ratio C 3.8 Si 1.8	As Cast	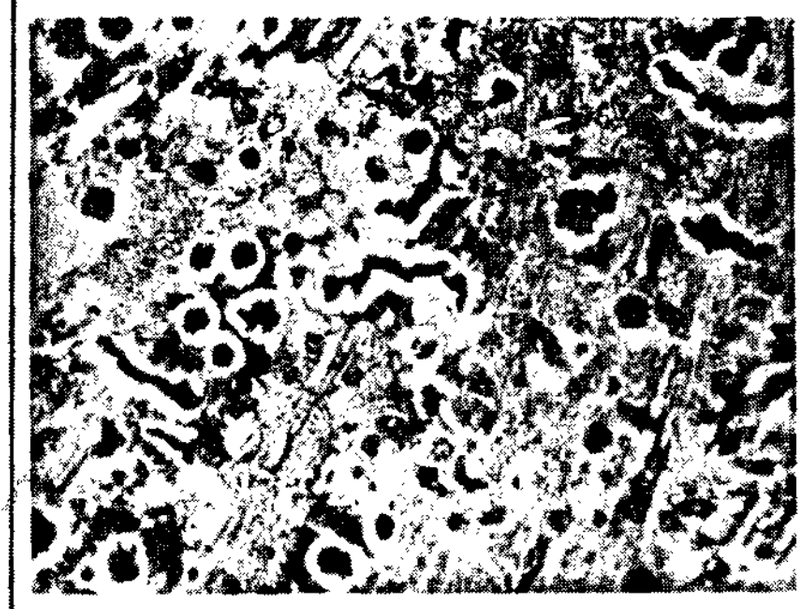	
	After Annealing	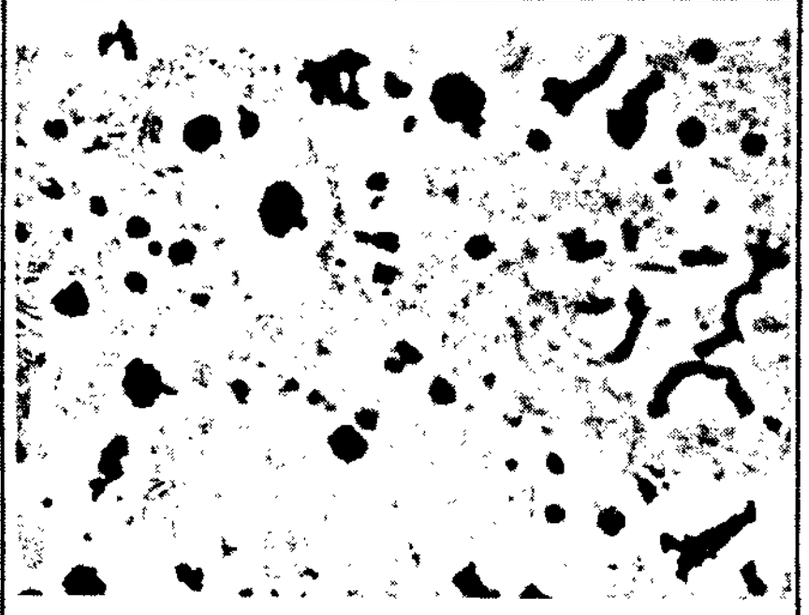	
C/Si Ratio C 3.4 Si 3.0	As Cast	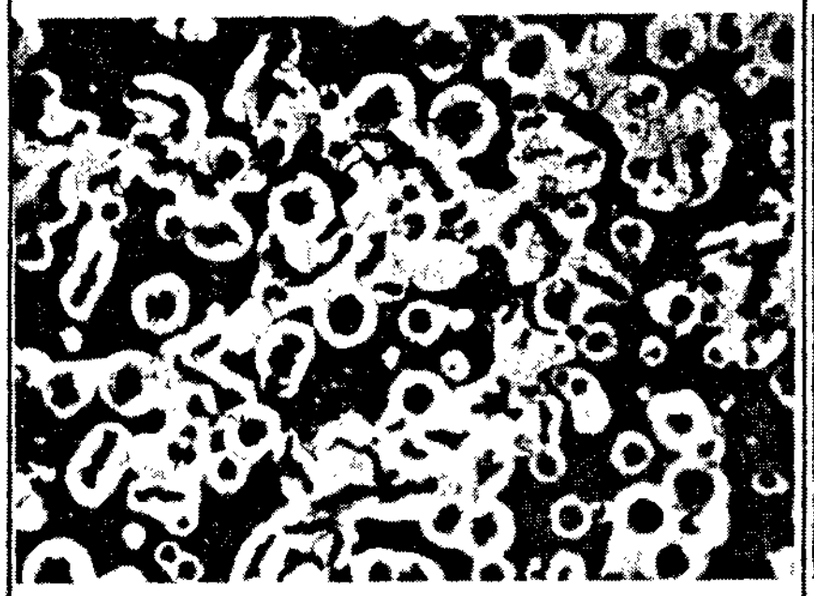	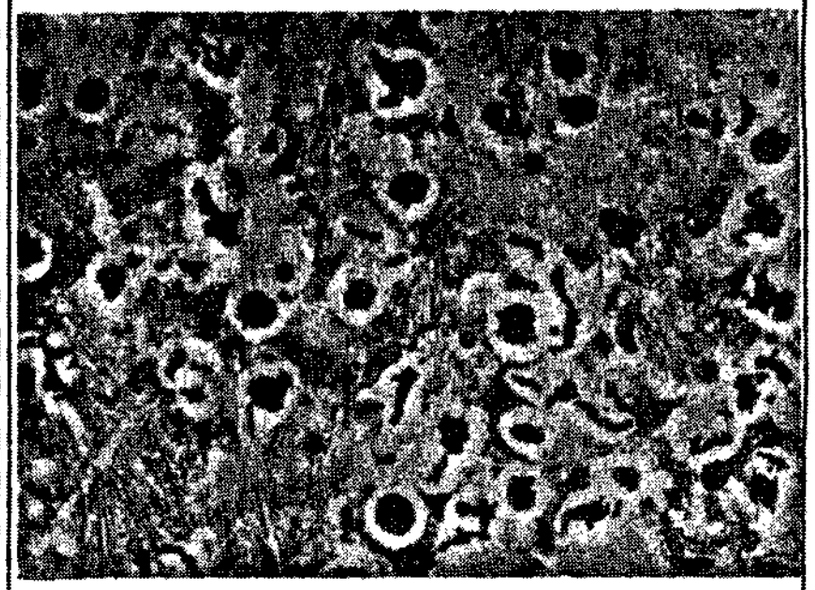
	After Annealing	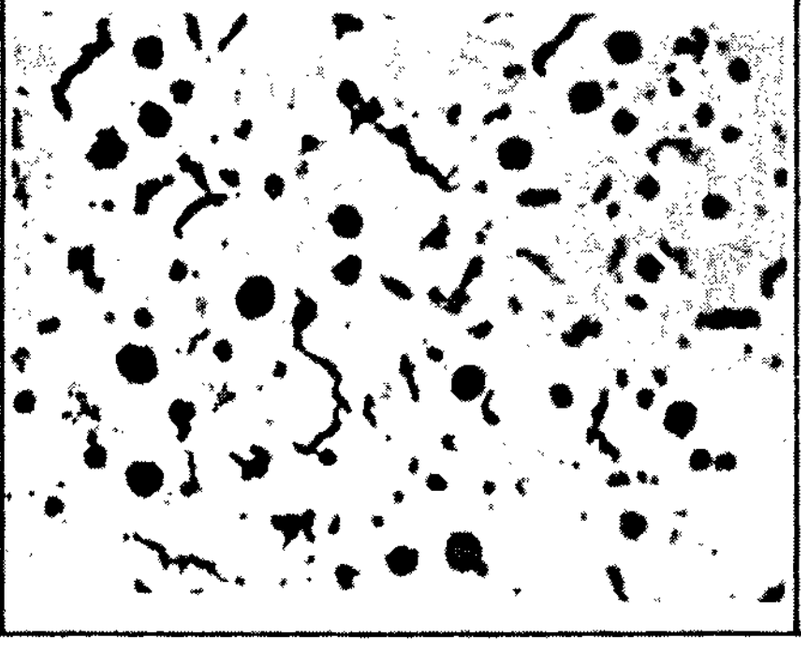	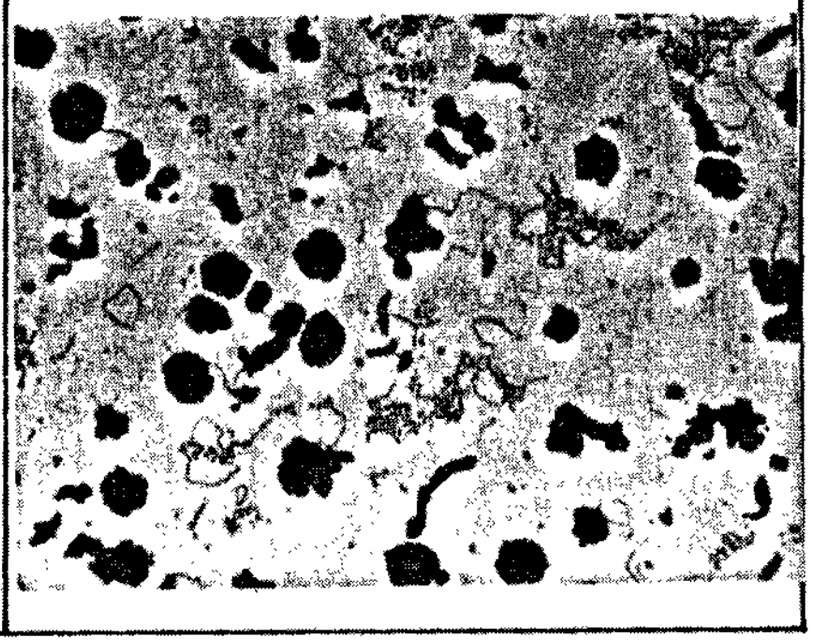

Fig. 6 Microstructures of cast iron, 12.5mm section size 0.5 min. holding time. (X150)

		Holding Time 0.5min.	Holding Time 4.5min.
Section Size 1.5inch 75X	As Cast	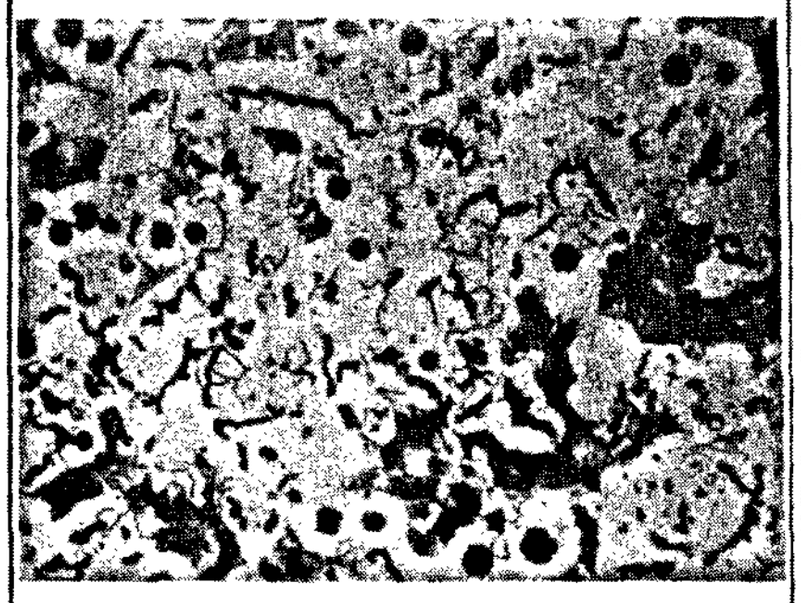	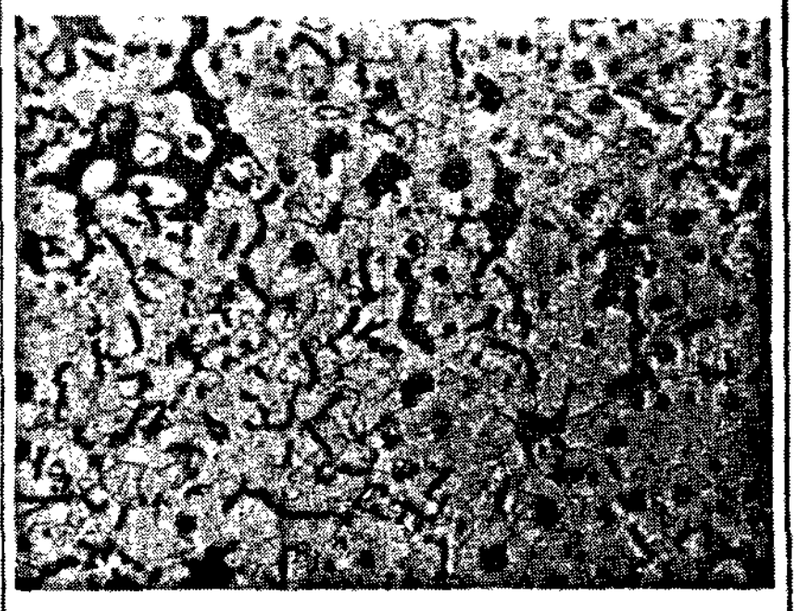
	After Annealing	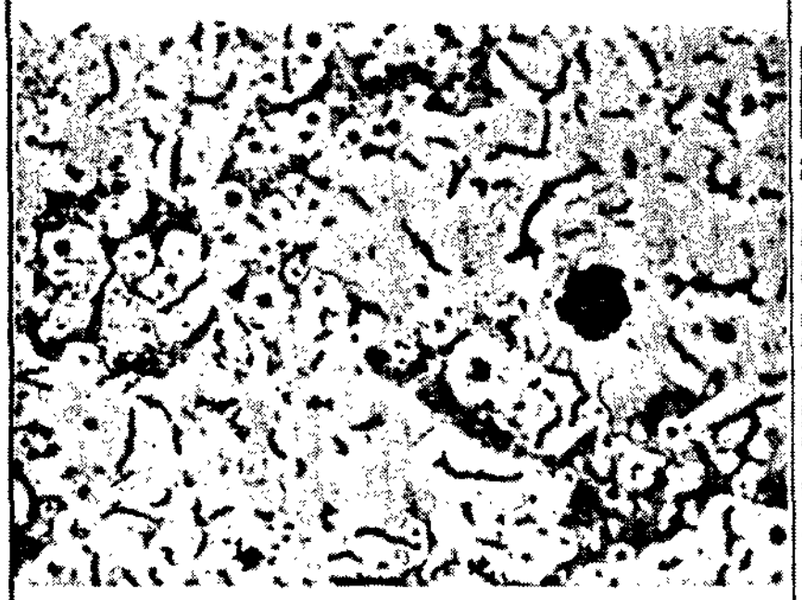	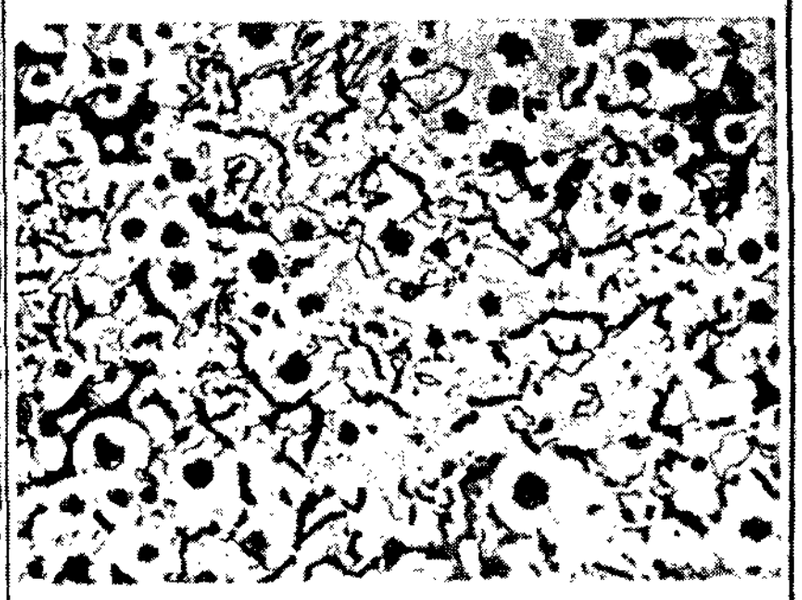
Section Size Left 1.0inch	As Cast	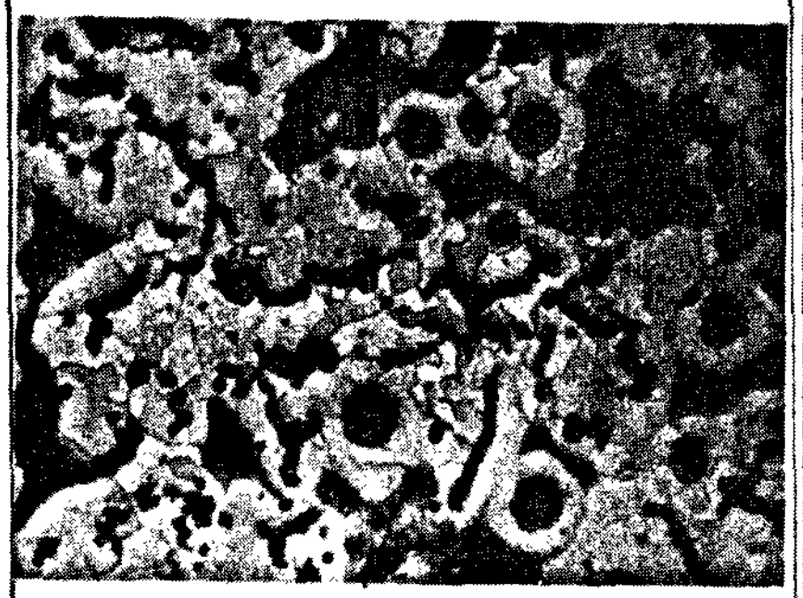	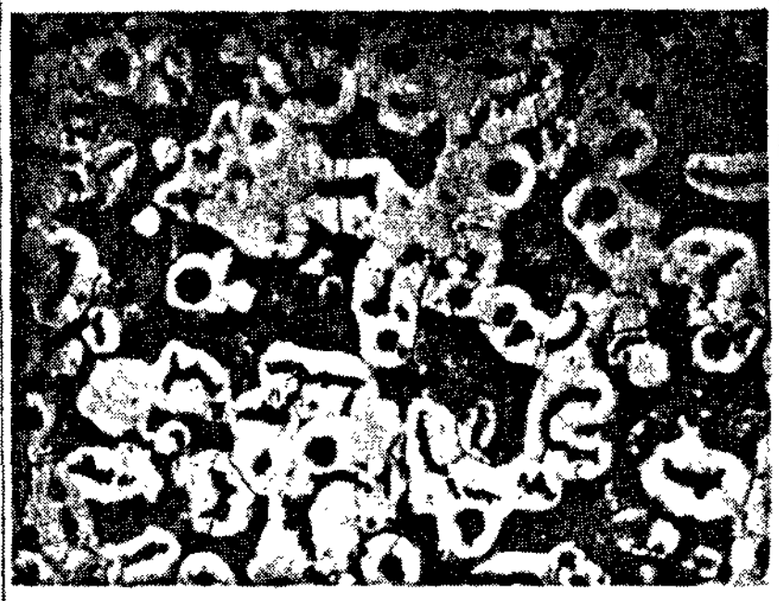
Right 0.5inch 150X	After Annealing	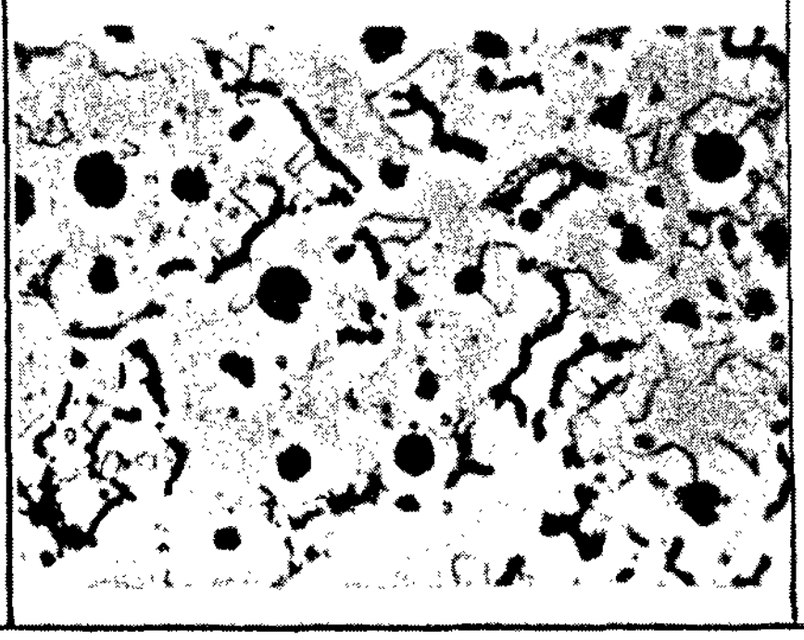	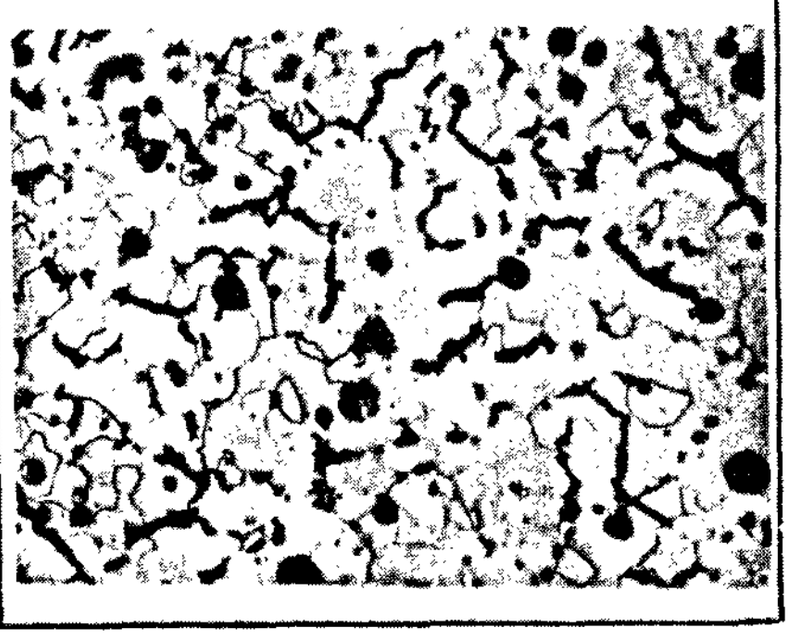

Fig. 7 Microstructures of Mg-Ti alloy treated cast iron C 3.4/Si 3.0

		Holding Time 0.5min.	Holding Time 4.5min.
Section Size 1.5inch 75X	As Cast		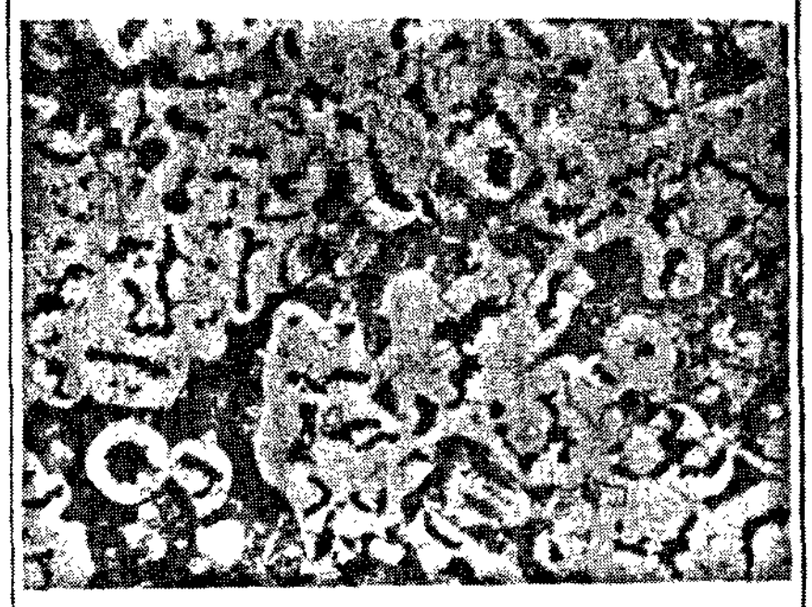
	After Annealing	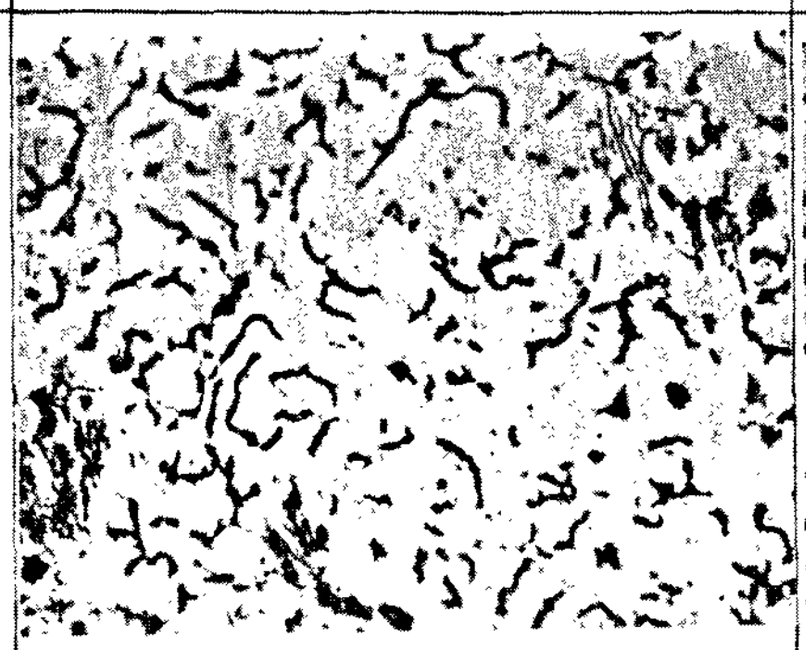	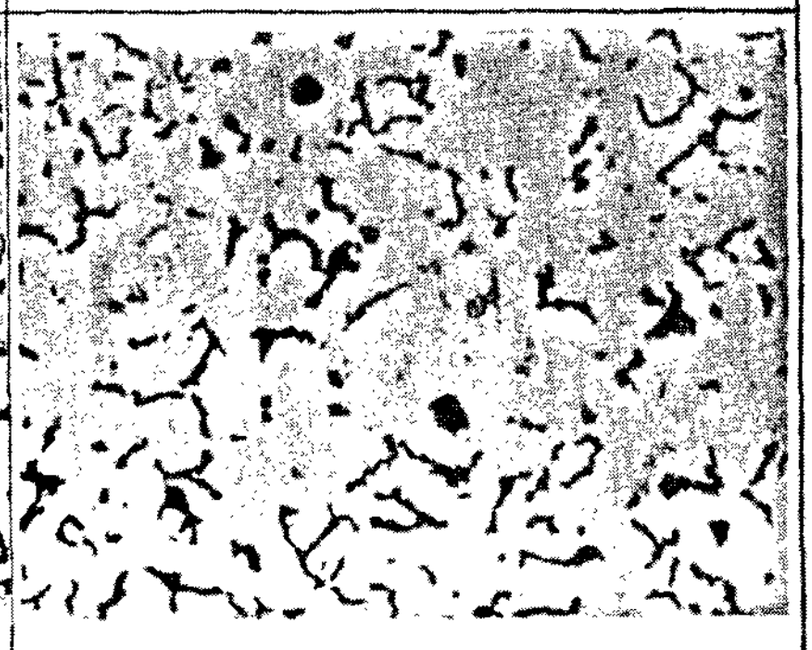
Section Size Left 1.0inch Right 0.5inch 150X	As Cast	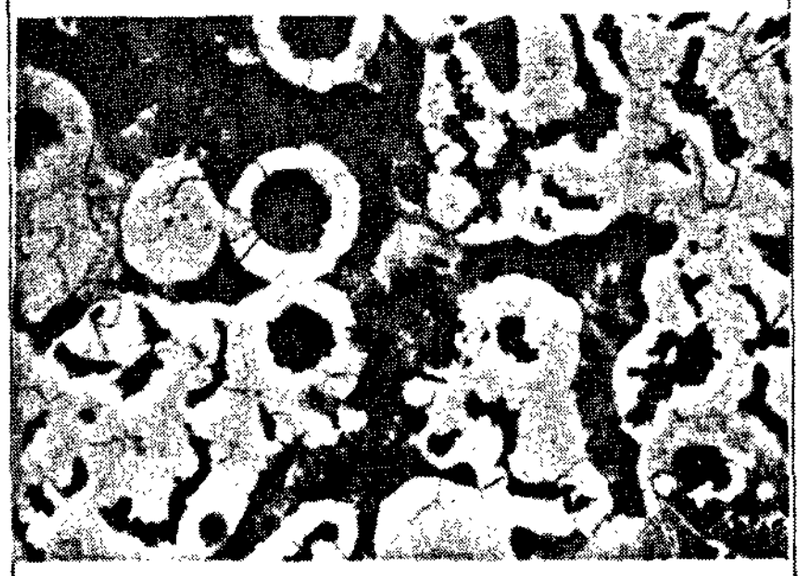	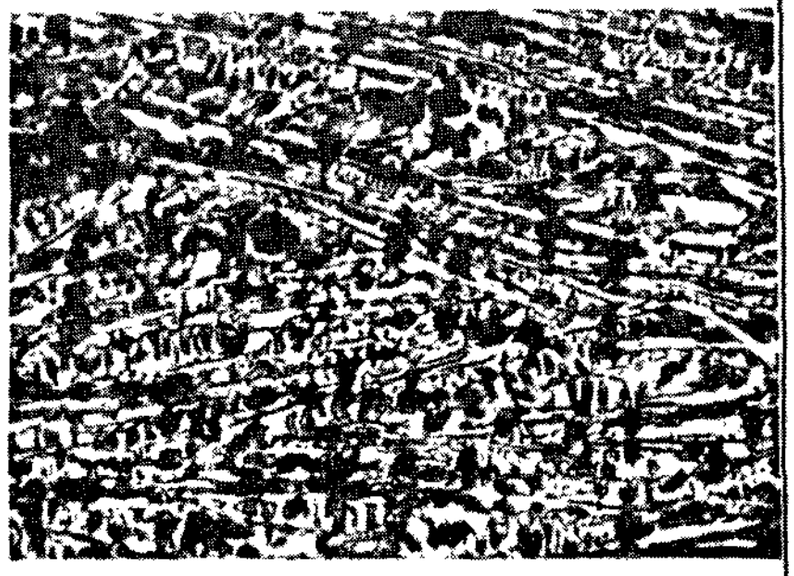
	After Annealing	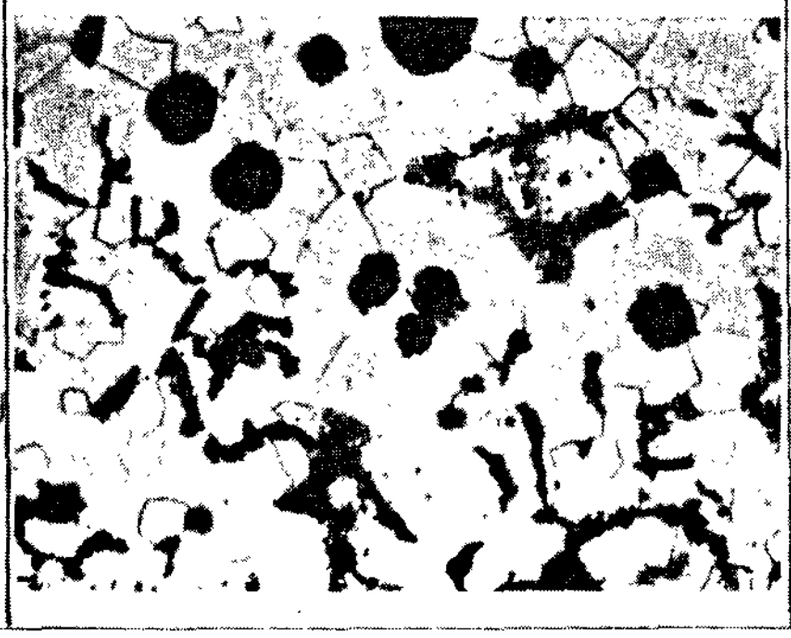	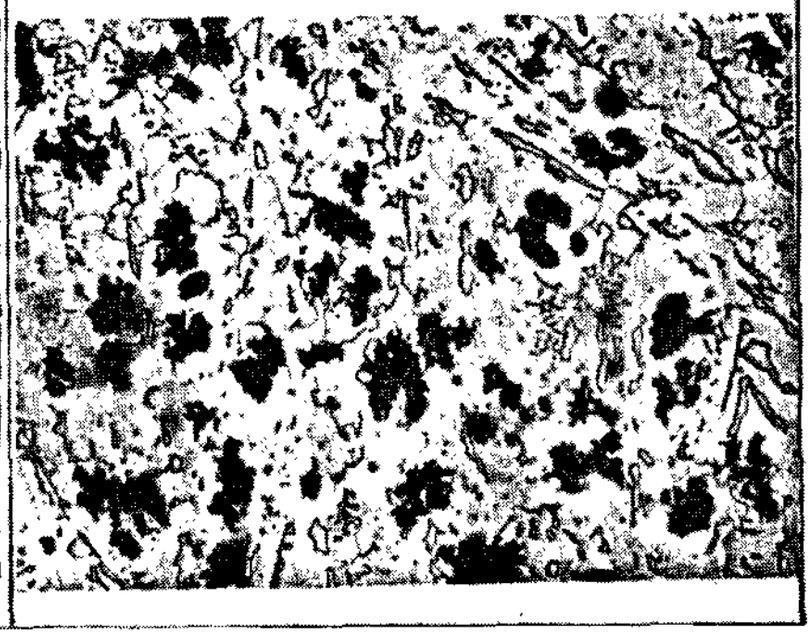

Fig. 8 Microstructures of rare earth silicide treated cast iron C 3.4/Si 3.0

5. Conclusions

1. A maximum holding time of 4.5 minutes is not enough to observe whether there is any effect of the holding time on the morphology of compacted graphite. However, it can be said that holding times up to 4.5 minutes do no affect the morphology of compacted graphite.

2. Rare earth silicides treated compacted graphite cast iron is more easily affected by annealing than Mg-Ti alloy treated irons. In other words, the Mg-Ti alloy treated compacted graphite does not change its shape even after annealing(1 hour, 871 C, furnace cooling).

Rare earth treated compacted graphite in a thin section sample(13mm) becomes slightly thicker and longer during annealing due to graphitization.

References

1. C. R. Loper Jr., et al. : 46th International Foundry Congress. Madrid, Spain(1979)
2. K. P. Cooper, C. R. Loper Jr. : AFS Trans, Vol. 86(1978)
3. T. Kimura : Ph. D. Thesis, University of Wisconsin Madison(1980)
4. C. R. Loper Jr., et al. : AFS Trans, Vol. 84 (1976) 203－214
5. J. F. Janowak and C. R. Loper Jr. : AFS Trans, Vol. 79(1971) 433－444